ELSEVIER

Journal of University of Science and Technology Beijing
Volume 15, Number 4, August 2008, Page 509

Materials

Damping properties of fly ash/epoxy composites

Jian Gu, Gaohui Wu, and Xiao Zhao

School of Materials Science and Engineering, Harbin Institute of Technology, Harbin 150001, China
(Received 2006-09-14)

Abstract: An inexpensive fly ash (FA), which is from a waste product, was employed to prepare fly ash/epoxy composites. The purpose of this study is to characterize the contributions of matrix viscoelasticity, hollow structure characteristic (porosity), and filler/matrix interface friction to the high vibration damping capacity of such composites. The damping properties of the composites were investigated in the temperature range of −40 to 150°C and in the frequency range of 10 to 800 Hz by using a tension-compression mode. The results indicate that the peak value of damping loss factor (tanδ) for the fly ash/epoxy composites can reach 0.70-0.90 in test specification, and the attenuation of damping loss factor is inconspicuous with increasing frequency. In addition, scanning electron microscope (SEM) was used to observe the morphology of the fly ash as well as its distribution in the matrix, which will help to analyze the effect of fly ash on the damping properties of the fly ash/epoxy composites.

Key words: composites; epoxy; fly ash; damping property; loss factor

1. Introduction

In aerospace and many other lightweight structures, there are many vibration inputs that can lead to resonance [1], so it is necessary to have a sound methodology to control the vibration. During the past few decades, it has become technically and ecologically important to suppress vibrational and impact noise [2]. From this scope, many mechanical dampers have been investigated and developed, and there, the exploitation of damping materials is a key point to produce efficient damping to eliminate vibration and noise [2-3]. In particular, the polymer composite, as a novel damping material, has attracted great interest in the development because of its excellent stiffness and damping characteristics [4].

In recent years, research on fly ash as a filler and reinforcement in metal-matrix composites (MMCs) and polymer-matrix composites (PMCs) has been growing [5-7]. Fly ash particles can be classified into two types, cenosphere and precipitator. Generally, the solid spherical particles of fly ash are called precipitator fly ash, and the hollow particles of fly ash with a density less than 1.0 g·cm^{-3} are called cenosphere fly ash [7]. The cost, when bought in large quantities, is very low because fly ash is a by-product of coal combustion, and there are many advantages such as low density, strong filling ability, excellent fluidity, and good processibility of the filled materials [8]. Moreover, there are few studies on the relationship between damping behavior and a composite filled with fly ash, but its internal micropore structure may help vibration damping and noise absorption.

As a way of investigating the effect of fly ash on damping properties, the authors have aimed at fly ash/polymer composites as damping materials. In this article, new types of damping materials which are composed of fly ash and modified epoxy resin are introduced.

2. Experimental

2.1. Materials

Epoxy resin (A-component: epoxy resin E-51; B-component: solidified agent, accelerant, *et al.*); polyurethane (A-component: polyethylene glycol; B-component: Tolylene-2, 4-diisocyanate, and polyethylene glycol, catalyst, accelerant); ethyl acetate, epoxy propane butyl ether (diluting agent); γ-aminopropyl triethoxy silane (silane coupling agent).

The fly ash originating from coals is typical of that

Corresponding author: Jian Gu, **E-mail:** gujian9804@163.com

burned in electric power plants. The density of cenosphere fly ash is about 0.57-0.70 g·cm^{-3}, and that of precipitator fly ash is about 1.90 g·cm^{-3}. The surface of fly ash particles was coated with a cross-linked silane film, except where indicated otherwise.

2.2. Composite preparation

The predetermined proportions (wt%) of epoxy resin and its modifiers, additives, and fly ash were put into a beaker first. After that the materials were simply mixed and were blended in the melt state with an agitator at 60°C. Subsequently, they were dispersed with an ultrasonic instrument and degassed. Finally, the blended mixtures were cured at 60°C for 5 h and then postcured at 80°C for 10 h.

2.3. Apparatus and methodology

A morphological study was carried out by using a scanning electron microscope (SEM), model type S-4700, made by Hitachi (Japan), to observe the distribution of fly ash in the matrix and the interface adhesion between fly ash particles and the matrix.

Fourier transform infrared spectrum (FT-IR) analysis was performed on a Perkin-Elmer one series FT-IR spectrometer with 4 cm^{-1} resolution. The samples were mixed with dry, powdery KBr, pelletized under pressure and then scanned. The scanning speed was 0.2 cm·s^{-1} and the samples were measured in the range of 4000-370 cm^{-1} as KBr pellets.

The main apparatus used in the damping capacity test was a dynamic mechanical analyzer, the MAK-04 Viscoanalyzer (France). The tension-compression mode was employed and the dimensions (length, width, and thickness) of the specimen were about 30, 5, and 1.5 mm, respectively. The temperature dependence of tanδ was measured from −40°C to 150°C at a heating rate of 3°C/min with a frequency of 30 Hz. The frequency dependence of tanδ was measured from 10 to 800 Hz at the glass transition temperature (T_g) in an argon atmosphere.

3. Results and discussion

3.1. Morphology

Fig. 1 shows the SEM photographs of cenosphere fly ash and precipitator fly ash. From Fig. 1(a), it can be seen that cenosphere fly ash is a regular, spherical particle and there are farthing micropores on the surface. The hollow structure with the porous center of cenosphere fly ash is consecutive entirety, and the thickness of the pore's shells is about 4-10 μm [9]. However, the spherical shape of precipitator fly ash is not very regular, and there are many anomalous micropores on the surface. The hollow structure of precipitator fly ash is inconsecutive, and the micropores consist of a spot of closed pores and many open pores, as depicted in Fig. 1(b).

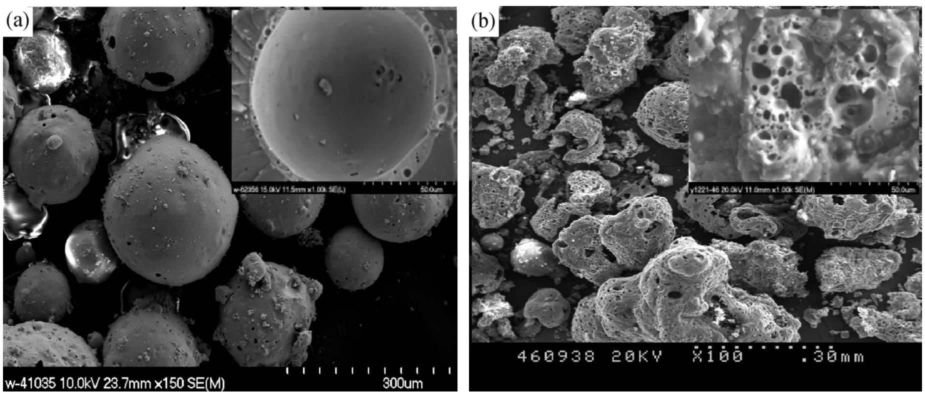

Fig. 1. SEM photographs: (a) cenosphere fly ash; (b) precipitator fly ash.

Fig. 2 presents the fractographs of the composites filled with cenosphere fly ash and precipitator fly ash. From Fig. 2(a), it can be seen that the cenosphere fly ash particles disperse and distribute into the matrix uniformly, and the particles can be seen clearly except a few particle-rich regions. However, in Fig. 2(b), obvious precipitator fly ash particles in the epoxy matrix cannot be seen, which may be ascribed to a good interfacial adhesion between the precipitator fly ash particles and the matrix, and there are many anomalous micropores on the surface of the fly ash. The precipitator fly ash particles are mostly infiltrated by a great deal of epoxy matrix, thus leading to a large elimination of the micropores. These results indicate that the micropores on the surface of the precipitator fly ash must be extended into the inner.

3.2. Infrared spectrum analysis

Fig. 3 presents the FT-IR spectra for γ-aminopropyl triethoxy silane and the fly ash particles with and without surface treatment. In Fig. 3(a), the curve denotes the characteristic peak of γ-aminopropyl triethoxy silane. The band lying around 2978 cm^{-1} represents a vibration absorbing peak of the C–H bond, which belongs to $-CH_3$. In Fig. 3(b), the fly ash particles without surface treatment have a very intensive band, which is related to the vibration absorbing peak of the –Si–O–Si– group, at 1095 cm^{-1} [10-11], and the absorbing peak lying at 3426 cm^{-1} is caused by the flexible vibration of the hydroxyl group (–OH) [10]. In Fig. 3(c), there are a few new absorbing peaks of the fly ash particles with surface treatment occurring at 2980, 2888, 1520, 1450, 1372, and 736 cm^{-1}, but these peaks are absent in the spectra of the fly ash particles without surface treatment, which suggests that these peaks correspond to the characteristic peaks of γ-aminopropyl triethoxy silane. Herein, the peak lying between 2888 and 2980 cm^{-1} represents the characteristic peak of the C–H bond. Additionally, the peak lying at 3426 cm^{-1} weakens, which indicates that the quantity of the hydroxyl group (–OH) reduces, and reactions must take place between the γ-aminopropyl triethoxy silane and the hydroxyl group on the surface of the fly ash particles.

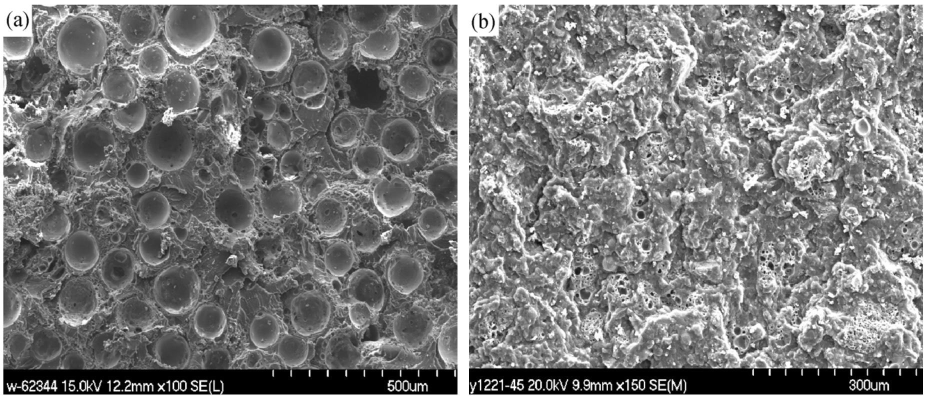

Fig. 2. Fractographs of the composites filled with cenosphere fly ash (a) and precipitator fly ash (b).

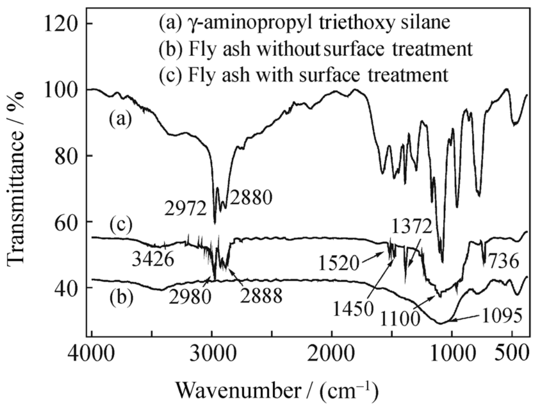

Fig. 3. FT-IR spectra for γ-aminopropyl triethoxy silane (a), the fly ash without (b) and with (c) surface treatment.

The basic principle of surface treatment with γ-aminopropyl triethoxy silane can be interpreted as follows: γ-aminopropyl triethoxy silane [12-13] with the general chemical structure $(RO)_3SiY$, where –RO is an alkoxy group and –Y is an organic-functional group. During the surface treatment of fly ash particles with γ-aminopropyl triethoxy silane, the alkoxy group hydrolyzes in an aqueous environment, producing the hydroxyl group, one or more of which condense with the hydroxyl groups commonly found on the surfaces of fly ash particles. Subsequent drying leads to the formation of both covalent bond linkages with the surfaces of fly ash particles and the development of a cross-linked silane film, which may be in favor of improving the resin-wettability. Therefore, it can be concluded that the effect of the silane coupling agent on the interfacial adhesion conditions between fly ash particles and the matrix is quite significant.

3.3. Density and porosity

The Archimedes' drainage method is initially used to measure the volume of the composites (V), after which the mass of the composites (M) is quantified by an analytical balance, and finally, the density of the composites (ρ_c) can be figured out. Furthermore, the porosity of the composites can be calculated through the following equations:

$$V_h = \left(1 - V_f - \frac{\rho_c - \rho V_f}{\rho_m}\right) \times 100\% \tag{1}$$

$$\theta = V_h + (1 - \frac{\rho}{\rho_s})V_f \tag{2}$$

where θ is the porosity, V_f and V_h are the volume fraction of the fly ash and holes originating from the curing process, and ρ_s, ρ_m, and ρ are the densities of the pore shells, the matrix, and the fly ash, respectively.

The data of V_f, density, and porosity of the composites are listed in Table 1. From Table 1, it can be identified that the density and porosity of the cenosphere fly ash/epoxy composite are 1.120 $g\cdot cm^{-3}$ and 26.0vol%, and those of the precipitator fly ash/epoxy composite are 1.484 $g\cdot cm^{-3}$ and less than 6.4vol%, respectively.

3.4. Effect of different types of fly ash on damping

The loss factor ($\tan\delta$) is the most basic measurement approach of the damping capacity of materials. The temperature dependence of tanδ of the epoxy composites filled with different types of fly ash, at 30 Hz, is shown in Fig. 4. From this figure, it can be seen that the peak values of tanδ of the fly ash/epoxy composites are higher than those of the epoxy matrix, and the glass transition temperature shifts to the direction of low temperature. The peak value of tanδ of the composite filled with cenosphere fly ash is slightly higher than that of the composite filled with precipitator fly ash, and the damping temperature regions that refer to the temperature range of tanδ more than 0.5, are about 8, 40, and 69°C, respectively, for the three materials. These results all indicate that the composite filled with cenosphere fly ash has a relatively better damping property within the three materials. Besides, the damping properties of the two composites are both obviously better than that of the matrix.

Table 1. Data of V_f, density, and porosity of the composites

Samples	V_f / vol%	ρ_m / (g·cm^{-3})	ρ / (g·cm^{-3})	ρ_s / (g·cm^{-3})	ρ_c / (g·cm^{-3})	θ / vol%
Cenosphere FA/epoxy composite	30	1.416	0.614	2.320	1.120	26.0
Precipitator FA/epoxy composite	30	1.416	1.900	2.482	1.484	<6.4

The frequency dependence of tanδ of the epoxy composites filled with different types of fly ash, at T_g, is shown in Fig. 5. From the curves, it can be seen that the frequency dependence of tanδ of the type of fly ash is similar to the situation displayed in Fig. 4. The initial tanδ values of the composites filled with cenosphere fly ash and precipitator fly ash are 0.81-0.90 and 0.77-0.88, respectively, in the test frequency range of 10-100 Hz, which are higher than that of the matrix (0.48-0.56). With increasing frequency in the range of 100-800 Hz, the attenuation of tanδ is inconspicuous, and the value of tanδ of the composite filled with cenosphere fly ash is nearly twice that of the matrix.

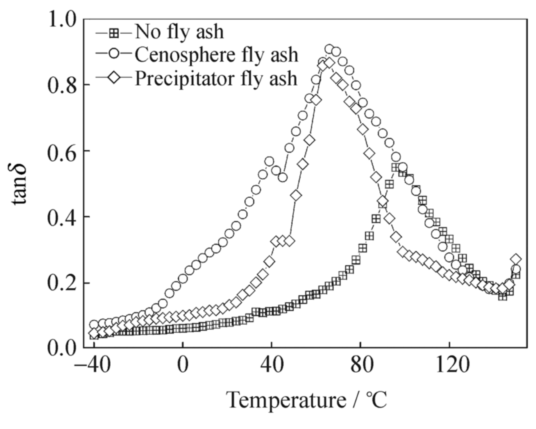

Fig. 4. Temperature dependence of tanδ of the composites filled with different types of fly ash.

The damping mechanisms of the composites include not only the contribution of matrix viscoelasticity, but also grain boundary sliding (filler/filler) and interfacial sliding (filler/matrix) friction [14]. Moreover, the effect of the hollow structure on damping is one of the important factors. Relative to the matrix, the composite filled with cenosphere fly ash has many contributions coming from the frictional loss and the hollow structure, which may remarkably increase the damping capacity. However, for the composite filled with precipitator fly ash, which also has an excellent damping capacity, the hollow structure is rare. The analysis results show that numerous contributions to damping capacity is from the frictional loss except the matrix viscoelasticity, and the reason may be that the precipitator fly ash particles are mostly infiltrated by a great deal of epoxy matrix, and the two phases differ greatly in the dynamic modulus, leading to large strain phasic discrepancy, and promoting the phase lagging between the stress and the strain, consequently enhancing the loss factor of this composite [15].

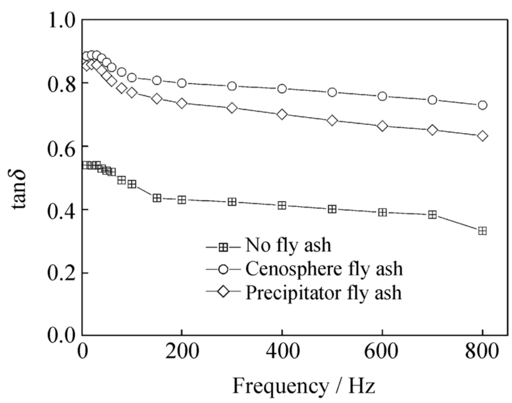

Fig. 5. Frequency dependence of tanδ of the composites filled with different types of fly ash.

4. Conclusions

(1) The density and porosity of the cenosphere fly ash/epoxy composite are 1.120 g·cm^{-3} and 26.0vol%, and those of the precipitator fly ash/epoxy composite are 1.484 g·cm^{-3} and less than 6.4vol%, respectively.

(2) Cenosphere fly ash and precipitator fly ash have different microstructures. Thereinto, cenosphere fly ash is a regular spherical particle with farthing micropores on the surface, but these micropores of precipitator fly ash are separated by thin pore shells. The cenosphere fly ash particles distribute into the matrix uniformly and the particles can be seen clearly,

whereas, the precipitator fly ash particles are mostly infiltrated by a great deal of matrix resin and have good interfacial adhesion with the matrix.

(3) Both the temperature and frequency dependences of tanδ of the composites filled with different types of fly ash are in a similar situation. The composites filled with cenosphere fly ash and precipitator fly ash have much better damping properties than the matrix, and the damping property of the composite filled with cenosphere fly ash is slightly higher than that of the composite filled with precipitator fly ash.

References

[1] R.D. Adams and M.R. Maheri, Damping in advanced polymer-matrix composites, *J. Alloy. Compd.*, 355(2003), No.1-2, p.126.

[2] M. Hori, T. Aoki, Y. Ohira, *et al.*, New type of mechanical damping composites composed of piezoelectric ceramics, carbon black and epoxy resin, *Compos. Part A*, 32(2001), No.2, p.287.

[3] E.R. Michael, Dynamics of two-dimensional composites of elastic and viscoelastic layers, *J. Acoust. Soc. Am.*, 112(2002), No.3, p.1445.

[4] I.C. Inegan and R.F. Gibson, Recent research on enhancement of damping in polymer composites, *Compos. Struct.*, 44(1999), No.2-3, p.89.

[5] P.K. Rohtagi, R. Guo, B.N. Keshevaram, *et al.*, Research on fly ash as a filler and reinforcement in composites, [in] T.J. Srivatsan and J.T. Moore eds, *Proceedings of International Symposium on Processing and Fabrication of Advanced Materials IV*, *ASM International*, Cleveland, 1995, p.889.

[6] K.S. Rebeiz, J.W. Rosett, and A.P. Craft, Strength properties of polyester mortar using PET and fly ash wastes, *J. Energy Eng.*, 122(1996), No.2-3, p.10.

[7] T. Matsunage, J.K. Kim, S. Hardcastle, *et al.*, Crystallinity and selected properties of fly ash particles, *Mater. Sci. Eng. A*, 235(2002), No.1-2, p.333.

[8] R.K.Y. Li, J.Z. Liang, and S.C. Tjong, Morphology and dynamic mechanical properties of glass beads filled low density polyethylene composites, *J. Mater. Process. Technol.*, 79(1998), No.1-3, p.59.

[9] T. Sakamoto, K. Shibata, K. Takanashi, *et al.*, Analysis of surface composition and internal structure of fly ash particles using an ion and electron multibeam microanalyzer, *Appl. Surf. Sci.*, 203-204(2003), p.764.

[10] S. Kang, S.I. Hong, C.R. Choe, *et al.*, Preparation and Characterization of epoxy composites filled with functionalized nanosilica particles obtained *via* sol-gel process. *Polymer*, 42(2001), No.3, p.879.

[11] R. Leboda, V.M. Gunko, M. Marciniak, *et al.*, Structure of chemical vapor deposition titania/silica gel, *J. Colloid Interface Sci.*, 218(1999), No.1, p.37.

[12] B. Mouanda, Grafting polyvinylimidazole onto silicon wafers *via* a copolymer of methacrylate epoxy and methacrylate-functional silane coupling agents, *Polymer*, 38(1997), No.21, p.5301.

[13] A.C. Miller and J.C. Berg, Effect of silane coupling agent adsorbate structure on adhesion performance with a polymeric matrix, *Compos. Part A*, 34(2003), No.4, p.327.

[14] J.H. Gu, X.N. Zhang, M.Y. Gu, *et al.*, Internal friction peak and damping mechanism in high damping 6061Al/SiC_p/Gr hybrid metal matrix composite, *J. Alloy. Compd.*, 372(2004), No.1-2, p.306.

[15] J.Y. Liu, P. Xu, and Y.H. Yu, Manufacturing and damping properties of the composite material of foam aluminum, *Coal Mine Mach.* (in Chinese), 5(2004), No.5, p.35.